# The magnetic fields of large Virgo cluster spirals. II[*]

M. Weżgowiec[1,2], M. Urbanik[1], R. Beck[3], K. T. Chyży[1], and M. Soida[1]

[1] Obserwatorium Astronomiczne Uniwersytetu Jagiellońskiego, ul. Orla 171, 30-244 Kraków, Poland
   e-mail: mawez@astro.rub.de
[2] Astronomisches Institut der Ruhr-Universität Bochum, Universitätsstrasse 150, 44780 Bochum, Germany
[3] Max-Planck-Institut für Radioastronomie, Auf dem Hügel 69, 53121 Bonn, Germany

**ABSTRACT**

*Context.* The Virgo cluster of galaxies provides excellent conditions for studying interactions of galaxies with the cluster environment. Both the high-velocity tidal interactions and effects of ram pressure stripping by the intracluster gas can be investigated in detail.
*Aims.* We extend our systematic search for possible anomalies in the magnetic field structures of Virgo cluster spirals in order to characterize a variety of effects and attribute them to different disturbing agents.
*Methods.* Six angularly large Virgo cluster spiral galaxies (NGC 4192, NGC 4302, NGC 4303, NGC 4321, NGC 4388, and NGC 4535) were targets of a sensitive total power and polarization study using the 100-m radio telescope in Effelsberg at 4.85 GHz and 8.35 GHz (except for NGC 4388 observed only at 4.85 GHz, and NGC 4535 observed only at 8.35 GHz). The presented two-frequency studies allow Faraday rotation analysis.
*Results.* Magnetic field structures distorted to various extent are found in all galaxies. Three galaxies (NGC 4302, NGC 4303, and NGC 4321) show some signs of possible tidal interactions, while NGC 4388 and NGC 4535 have very likely experienced strong ram-pressure and shearing effects, respectively, visible as distortions and asymmetries of polarized intensity distributions. As in our previous study, even strongly perturbed galaxies closely follow the radio-far-infrared correlation. In NGC 4303 and NGC 4321, we observe symmetric spiral patterns of the magnetic field and in NGC 4535 an asymmetric pattern.
*Conclusions.* The cluster environment clearly affects the evolution of its member galaxies via various effects. Magnetic fields allow us to trace even weak interactions that are difficult to detect with other observations. Our results show that the degree of distortions of a galaxy is not a simple function of the distance to the cluster center but reflects also the history of its interactions. The angle Θ between the velocity vector $v$ and the rotation vector $\Omega$ of a galaxy may be a general parameter that describes the level of distortions of galactic magnetic fields. Information about the motions of galaxies in the sky plane and their three-dimensional distribution, as well as information about the intracluster medium can also be obtained from the Faraday rotation analysis.

**Key words.** galaxies: clusters: general – galaxies: clusters: individual: Virgo – galaxies: general – galaxies: magnetic fields – radio continuum: galaxies

## 1. Introduction

In our previous study (Weżgowiec et al. 2007) of radio polarization in Virgo cluster spiral galaxies, we found a variety of environmental effects manifested as distorted structures of the galactic magnetic fields. These interactions have been previously investigated in H I (Cayatte et al. 1990, 1994, 2009) and the ionised medium (Chemin et al. 2006). Both data sets suggest that the environment significantly affects the interstellar medium (ISM) of cluster galaxies. Theoretical estimations and simulations of ram-ressure stripping effects have been performed by Vollmer et al. (2001), Schulz & Struck (2001), and Roediger & Brüggen (2008). Our observations confirmed that cluster galaxies interact with their environment, as well as proved that radio polarimetry is a very sensitive tool for studying these interactions. Only few galaxies have been previously observed (see Chyży et al. 2002; Soida et al. 1996; Vollmer et al. 2004; Chyży et al. 2006) and our present survey extends the database of magnetic properties of Virgo cluster spirals.

To enrich the quality of the statistical analysis and thus to allow studies of global trends, we extended our preliminary results presented in Weżgowiec et al. (2007) to obtain a statistically complete sample of Virgo cluster spiral galaxies. We therefore searched for galaxies with an optical diameter of at least 4.5 arcmin (at the assumed distance to the Virgo cluster of 17 Mpc) and a radio flux density of the emission from the disk exceeding 40 mJy at 1.4 GHz. This selection yielded 12 galaxies in total. Five of them (NGC 4438, NGC 4501, NGC 4535, NGC 4548, and NGC 4654) had been observed previously (Weżgowiec et al. 2007) and two more, NGC 4254 and NGC 4569, had been observed in other projects (Chyży et al. 2007, 2006, respectively). The remaining five galaxies (NGC 4192, NGC 4302, NGC 4303, NGC 4321, and NGC 4388) are the subject of this study. We also complete the observations of one galaxy from our previous sample – NGC 4535 – at 8.35 GHz providing data of higher resolution to study in greater detail the unusual asymmetry of polarized intensity found by us with sensitive low-resolution 4.85 GHz observations (see Weżgowiec et al. 2007).

Our observations of the second part of the complete sample were designed to search for cases of galaxy-cluster interactions in different parts of the Virgo cluster. This would help us to

---

**Table 1.** Basic astronomical properties and parameters of radio observations of studied galaxies.

| NGC | Morph. type[a] | Optical position[a] $\alpha_{2000}$ | $\delta_{2000}$ | Incl.[a] [°] | Pos. ang.[a] [°] | Dist. to Vir A [°] | Number of cov. | rms in final map [mJy/b.a.] TP | PI |
|------|------|------|------|------|------|------|------|------|------|
| 4192 | SABb | $12^h13^m48\overset{s}{.}3$ | $+14°53'57\overset{''}{.}7$ | 78 | 152.5 | 4.84 | $20^c$ $12^b$ | $0.3^c$ $0.7^b$ | $0.09^c$ $0.1^b$ |
| 4302 | Sc | $12^h21^m42\overset{s}{.}5$ | $+14°35'52\overset{''}{.}1$ | 90 | 177.5 | 3.12 | $18^c$ $11^b$ | $0.3^c$ $0.8^b$ | $0.07^c$ $0.08^b$ |
| 4303 | Sbc | $12^h21^m55\overset{s}{.}0$ | $+04°28'28\overset{''}{.}8$ | 26.3 | 162 | 8.2 | $20^c$ $14^b$ | $0.3^c$ $1.1^b$ | $0.08^c$ $0.1^b$ |
| 4321 | SABb | $12^h22^m55\overset{s}{.}0$ | $+15°49'21\overset{''}{.}3$ | 30 | 130 | 3.9 | $21^c$ $15^b$ | $0.3^c$ $0.8^b$ | $0.07^c$ $0.1^b$ |
| 4388 | Sb | $12^h25^m46\overset{s}{.}8$ | $+12°39'43\overset{''}{.}6$ | 82 | 91.3 | 1.26 | $12^b$ | $0.9^b$ | $0.1^b$ |
| 4535 | SBc | $12^h34^m20\overset{s}{.}4$ | $+08°11'52\overset{''}{.}3$ | 41.3 | 180 | 4.3 | $20^c$ | $0.3^c$ | $0.07^c$ |

**Notes.** [a] Taken from HYPERLEDA database – `http://leda.univ-lyon1.fr` – see Paturel et al. (1983); [b] at 4.85 GHz; [c] at 8.35 GHz.

**Table 2.** Integrated data of studied galaxies.

| NGC | $S_{4.85\,GHz}$ (TP) [mJy] | $S_{4.85\,GHz}$ (POL) [mJy] | % $p$ at 4.85 GHz | $S_{8.35\,GHz}$ (TP) [mJy] | $S_{8.35\,GHz}$ (POL) [mJy] | % $p$ at 8.35 GHz |
|------|------|------|------|------|------|------|
| 4192 | $35 \pm 2.6$ | $4 \pm 0.3$ | $11.4 \pm 1.3$ | $25 \pm 1.6$ | $2.6 \pm 0.3$ | $10.4 \pm 1.5$ |
| 4302 | $17.4 \pm 1.6$ | $1.7 \pm 0.2$ | $9.8 \pm 1.3$ | $14.2 \pm 1$ | $1.6 \pm 0.2$ | $11.3 \pm 1.7$ |
| 4303 | $171.8 \pm 9.3$ | $7.9 \pm 0.5$ | $4.6 \pm 0.4$ | $107.3 \pm 5.5$ | $8.7 \pm 0.6$ | $8.1 \pm 0.7$ |
| 4321 | $95.7 \pm 5.3$ | $6.3 \pm 0.5$ | $6.6 \pm 0.6$ | $68.3 \pm 3.6$ | $5.7 \pm 0.4$ | $8.3 \pm 0.7$ |
| 4388 | $78.7 \pm 4.8$ | $0.9 \pm 0.3$ | $1.1 \pm 0.4$ | – | – | – |
| 4535 | – | – | – | $22 \pm 1.5$ | $2.7 \pm 0.3$ | $12.3 \pm 1.7$ |

**Notes.** TP = total power flux density. POL = polarized flux density. % $p$ – polarization degree.

determine the extent to which the magnetic field distortions observed in our first study represent a general rule. Our present study will be used to construct a comprehensive database of magnetic structures of cluster spiral galaxies. Together with the data in other wavelengths it also will provide important clues about both the evolution and interactions of galaxies with the cluster environment. We also carry out X-ray studies of the Virgo cluster galaxies, the results of which will place tight constraints on the nature of the interactions of galaxies with the intracluster medium (ICM). Our first results were published in Weżgowiec et al. (2011), where we report the first detection of a hot gas halo around a Virgo cluster galaxy reminiscent of a Mach cone geometry. The thorough analysis of X-ray data from selected Virgo cluster galaxies will be presented in separate papers.

## 2. Observations and data reduction

The observations were performed between August 2005 and May 2006 using the 100-m Effelsberg radio telescope of the Max-Planck-Institut für Radioastronomie[1] (MPIfR) in Bonn. The basic astronomical properties of the observed objects and details of our observations are summarized in Table 1.

All galaxies except NGC 4535 were observed at 4.85 GHz using the two-horn (with a horn separation of 8′) system at the secondary focus of the radio telescope (see Gioia et al. 1982). Each horn was equipped with two total power receivers and an IF polarimeter resulting in four channels containing the Stokes parameters $I$ (two channels), $Q$ and $U$. The telescope pointing was corrected by performing cross-scans of a bright point source close to the observed galaxy. The flux density scale was established by mapping point sources 3C 138 and 3C 286 and using

the formulae of Baars et al. (1977). The galaxies NGC 4192, NGC 4302, NGC 4303, NGC 4321, and NGC 4535 were also observed at 8.35 GHz using the single horn receiver. At 4.85 GHz (dual system used), a number of coverages in the azimuth-elevation frame were obtained for each galaxy, as indicated in Table 1. At 8.35 GHz (single horn), we performed scans alternatively along the RA and Dec directions. The data reduction was performed using the NOD2 data reduction package (see Weżgowiec et al. 2007, for details). For construction of the polarized intensity and polarization angle maps, the $Q$ and $U$ maps were clipped at the $3\sigma$ level, taking into account the positive bias introduced by combining the maps.

To show the structure of the magnetic field projected onto the sky plane, we used apparent $B$-vectors defined as E-vectors rotated by 90°. This was a good approximation of the sky-projected orientation of large-scale regular magnetic fields, as in the regions of significant polarized intensity the observed Faraday rotation measures show that the plane of polarization can be rotated by no more than ~10 degrees at the observed wavelengths, which is on the order of uncertainties introduced by the discussed low resolution study (see Sect. 3.7).

## 3. Results

In Sects. 3.1–3.6, we present the radio maps of individual galaxies. Because of their higher resolution, we only show (when possible) the maps at 8.35 GHz. The integrated data for the galaxies are summarized in Table 2. The data includes total power and polarized flux densities obtained by integrating the signal in polygonal areas encompassing all the visible radio emission. From these data, the polarization degrees were obtained, which are presented in Table 2. Section 3.7 presents the
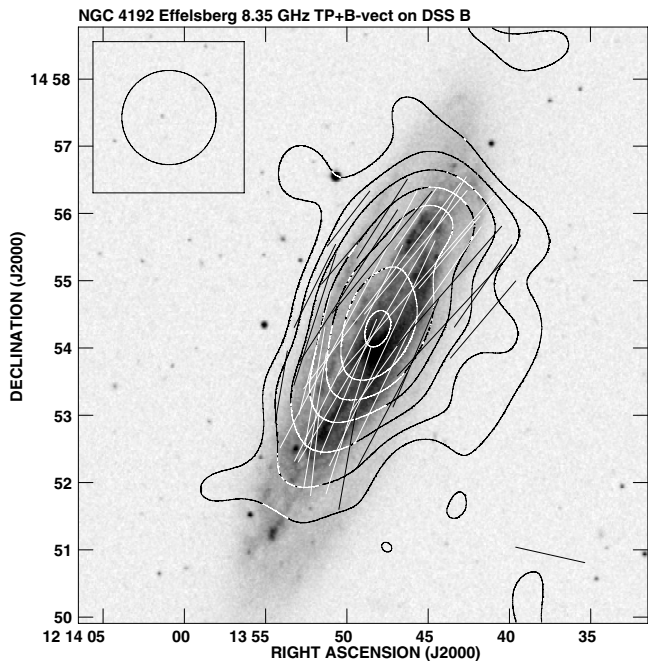
---

[1] `http://www.mpifr-bonn.mpg.de`

**Fig. 1.** Total power map of NGC 4192 at 8.35 GHz with apparent *B*-vectors of polarized intensity overlaid on the Digital Sky Survey (DSS) blue image. The contours are 3, 5, 8, 12, 16, 20, 25 × 0.3 mJy/b.a., and a vector of 1′ length corresponds to the polarized intensity of 0.25 mJy/b.a. The map resolution is 1′.5. The beam size is shown in the *top left* corner of the figure.
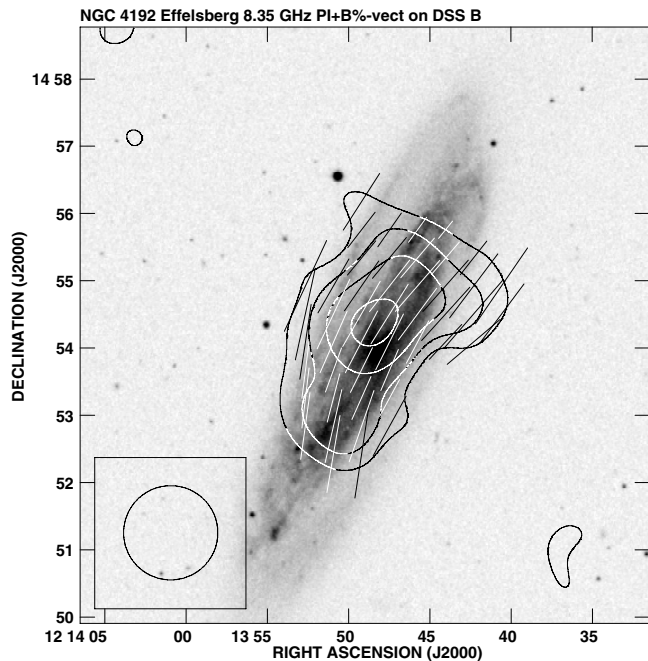
Faraday rotation measure maps obtained from our radio maps at 8.35 GHz and 4.85 GHz.

### 3.1. NGC 4192

NGC 4192 is an SABb edge-on galaxy located in the north-western outskirts of the cluster, about $4°.8$ (1.44 Mpc in the sky plane) from M 87 (Virgo A). The galaxy shows a warped H ɪ disk (Cayatte et al. 1990).

The total power peak almost coincides with the optical position of the galactic center (Fig. 1). On the western side of the galaxy disk, the total power extension can be seen. As checked using the NVSS data, this is not associated with point background sources. The polarization *B*-vectors are oriented roughly parallel to the disk in its inner parts. The apparent *B*-vectors in the outer parts of the disk (Fig. 2) show about a $30 \pm 10°$ inclination to the disk plane. Polarized emission comes mostly from the central parts of the disk and does not extend to the west by the same amount seen in the total power map. The alignment of the magnetic field vectors may indicate that the global magnetic field shows an X-shape structure, although it appears to be "flattened" on the eastern side of the disk. High resolution observations of this galaxy would be desirable to confirm such a magnetic-field structure.

### 3.2. NGC 4302

NGC 4302 is an edge-on Sc galaxy located in the cluster peripheries, about $3°.1$ (930 kpc in the sky plane) from Virgo A. It probably interacts with the neighboring galaxy NGC 4298 (Koopmann & Kenney 2004).

The map of total power intensity (Fig. 4) reveals an extension in the eastern direction. The galaxy visible at this position,
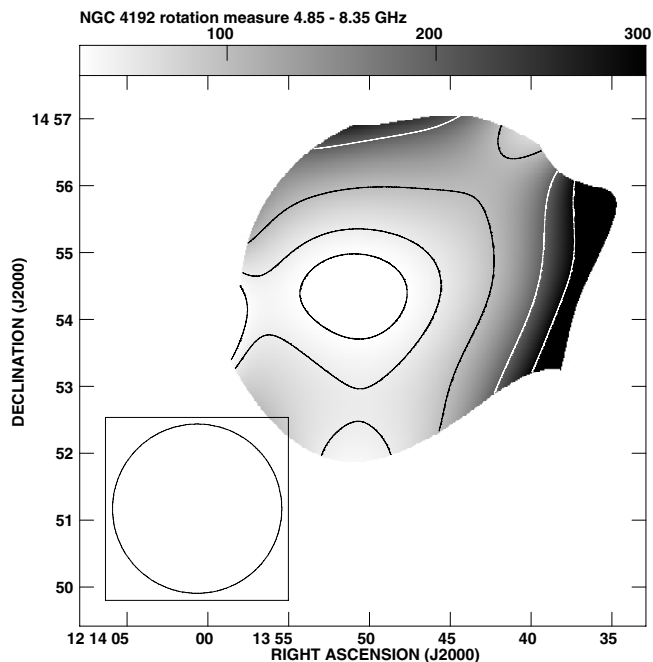


**Fig. 2.** Map of polarized intensity of NGC 4192 at 8.35 GHz with apparent *B*-vectors of polarization degree overlaid on the DSS blue image. The contours are 3, 5, 8, 13 × 0.09 mJy/b.a., and a vector of 1′ length corresponds to the polarization degree of 15%. The map resolution is 1′.5. The beam size is shown in the *bottom left* corner of the figure.



**Fig. 3.** Map of the rotation measure between 4.85 GHz and 8.35 GHz of NGC 4192. The contours are 3, 5, 10, 20, 30 × 10 rad/m². The map resolution is 2′.5. The beam size is shown in the *bottom left* corner of the figure.

PGC 169114 is not a source of measurable radio emission, as checked with NVSS and FIRST data. The polarization *B*-vectors in the disk plane of NGC 4302 are plane-parallel, while those further away to the east are inclined towards the extension.

An emission south of NGC 4298 is due to a background NVSS radio source J122131 + 143352 with total flux density (at 1.4 GHz) of 12.7 mJy (Condon 1998).
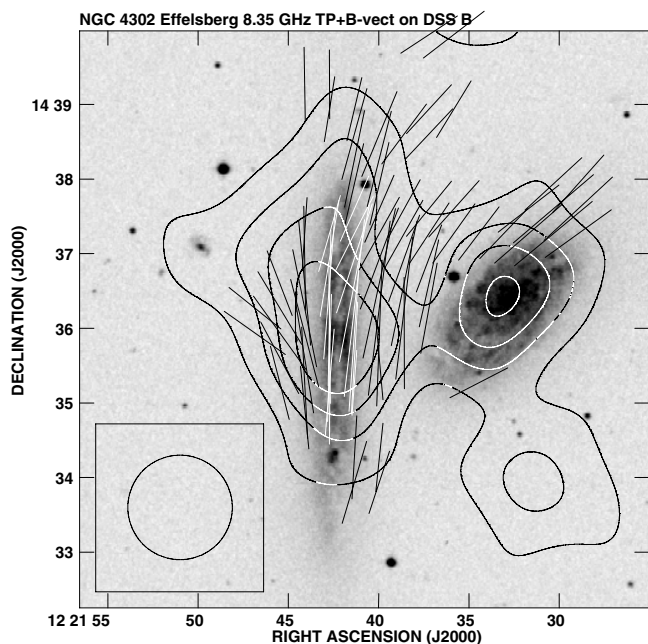
**Fig. 4.** Total power map of NGC 4302 and its companion NGC 4298 at 8.35 GHz with apparent *B*-vectors of polarized intensity overlaid on the DSS blue image. The contours are 3, 8, 12, 16 × 0.3 mJy/b.a., and a vector of 1′ length corresponds to the polarized intensity of 0.25 mJy/b.a. The map resolution is 1′.5. The beam size is shown in the *bottom left* corner of the figure.
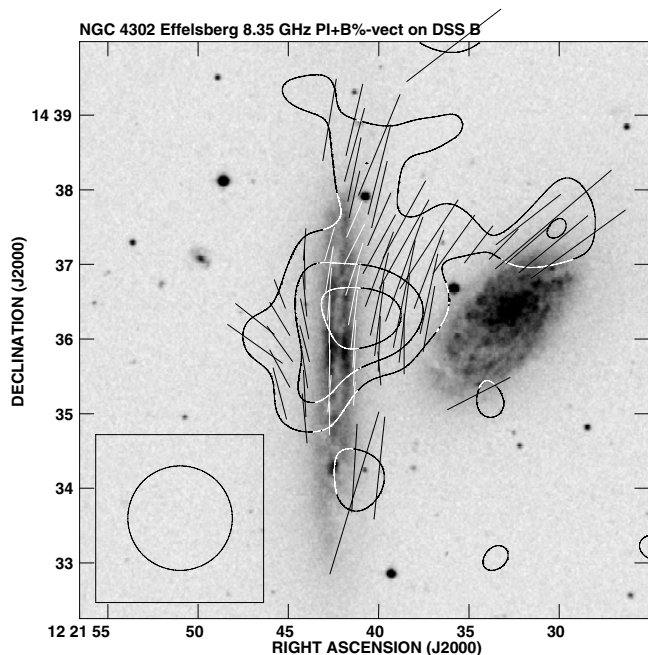


**Fig. 6.** Map of the rotation measure between 4.85 GHz and 8.35 GHz of NGC 4302 and its companion NGC 4298. The contours are −7, −1, 0, 1, 5, 7 × 20 rad/m$^2$. The map resolution is 2′.5. The beam size is shown in the *bottom right* corner of the figure.

likely caused by depolarization within the beam, as the galaxy is nearly face-on and the beamsize is roughly of the same size as the galaxy. A small patch of the polarized emission visible north of NGC 4298 and *B*-vectors aligned with the direction to NGC 4302 provide more arguments in favor of interactions between these two galaxies.

### 3.3. NGC 4303

NGC 4303 is a grand-design barred spiral of Sbc type located in the southern outskirts of the cluster, about 8°.2 (2.46 Mpc in the sky plane) from M 87. This galaxy an unperturbed H i and Hα distributions.

The total power emission (Fig. 7) is symmetrical having only slight extensions to the north and northwest. However, the latter extension is due to a background NVSS radio source J122143 + 042941, which has a total flux density of 15 mJy at 1.4 GHz. Another NVSS radio source J122154 + 042735 is visible south of the galaxy center. Its flux density at 1.4 GHz is as high as 16 mJy. The polarization *B*-vectors follow the spiral structure of the galaxy with somewhat higher pitch angles in the eastern part of the disk. On the map of polarized intensity (Fig. 8), two peaks can be seen in the interarm regions close to the galactic center. The peaks resemble highly polarized upstream regions in the barred galaxy NGC 1097 (Beck et al. 2005). There is an emission hole along the galaxy's bar due to a beam depolarization.



**Fig. 5.** Map of polarized intensity of NGC 4302 and its companion NGC 4298 at 8.35 GHz with apparent *B*-vectors of polarization degree overlaid on the DSS blue image. The contours are 3, 5, 7 × 0.07 mJy/b.a., and a vector of 1′ length corresponds to the polarization degree of 15%. The map resolution is 1′.5. The beam size is shown in the *bottom left* corner of the figure.

The peak of polarized intensity (Fig. 5) is shifted and elongated towards a companion galaxy with which it may interact tidally. The strongest polarized intensity is found in the region between galaxies. Although NGC 4298 is of the same Sc-type as NGC 4302, it lacks any polarized emission. This is most
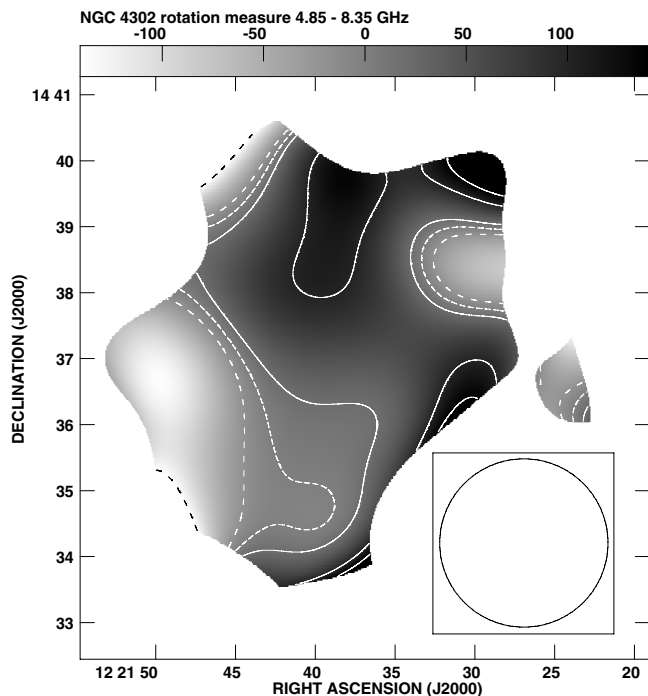
### 3.4. NGC 4321

NGC 4321 is another grand-design barred spiral galaxy of SABb type. It is located at the distance of 3°.9 from the cluster core to the north (1.17 Mpc in the sky plane), which places it in the
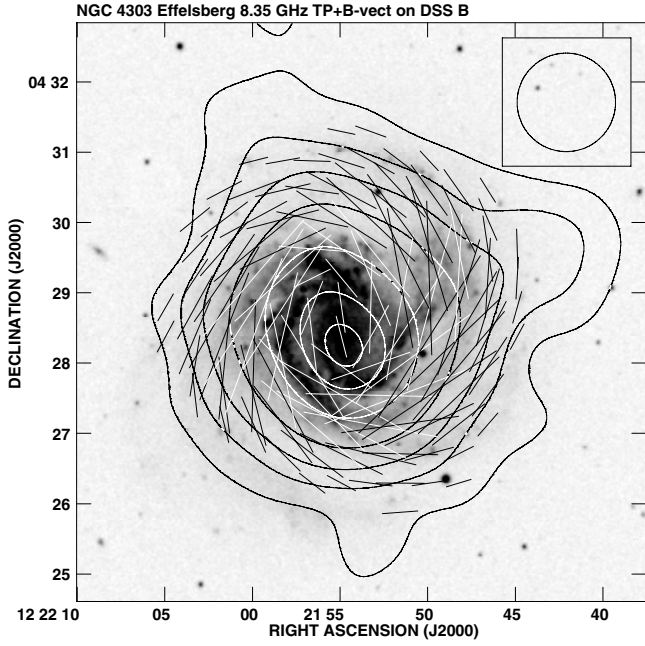
**Fig. 7.** Total power map of NGC 4303 at 8.35 GHz with apparent *B*-vectors of polarized intensity overlaid on the DSS blue image. The contours are 3, 8, 16, 32, 64, 96, 112 × 0.3 mJy/b.a., and a vector of 1′ length corresponds to the polarized intensity of 0.7 mJy/b.a. The map resolution is 1.′5. The beam size is shown in the *top right* corner of the figure.
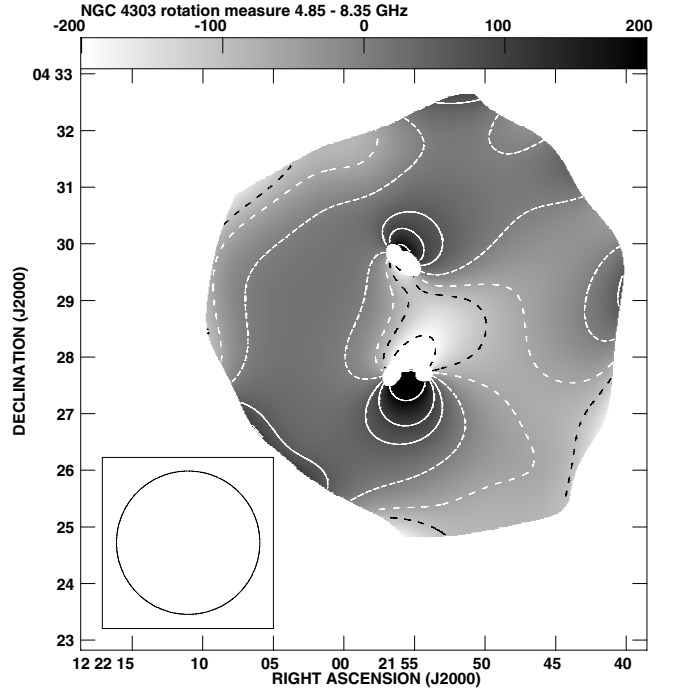


**Fig. 9.** Map of the rotation measure between 4.85 GHz and 8.35 GHz of NGC 4303. The contours are −10, −5, −3, 0, 3, 5, 10 × 20 rad/m². The map resolution is 2.′5. The beam size is shown in the *bottom left* corner of the figure.
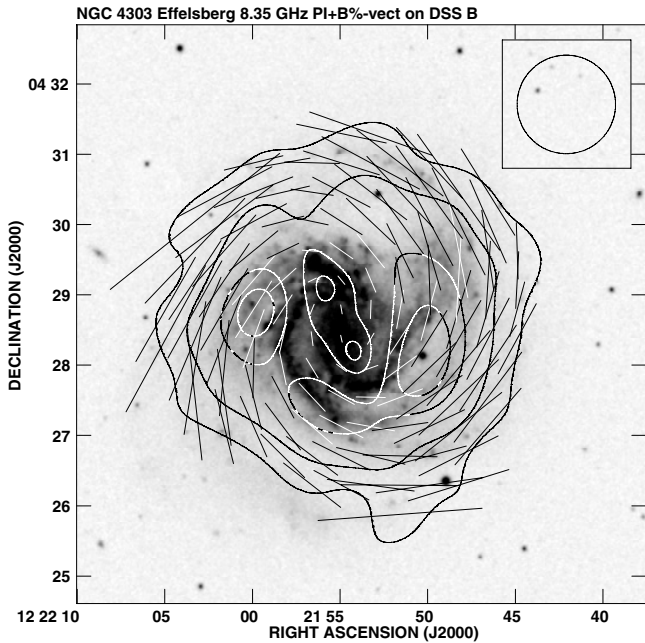


**Fig. 8.** Map of polarized intensity of NGC 4303 at 8.35 GHz with apparent *B*-vectors of polarization degree overlaid on the DSS blue image. The contours are 3, 8, 16, 20 × 0.08 mJy/b.a., and a vector of 1′ length corresponds to the polarization degree of 12%. The map resolution is 1.′5. The beam size is shown in the *top right* corner of the figure.
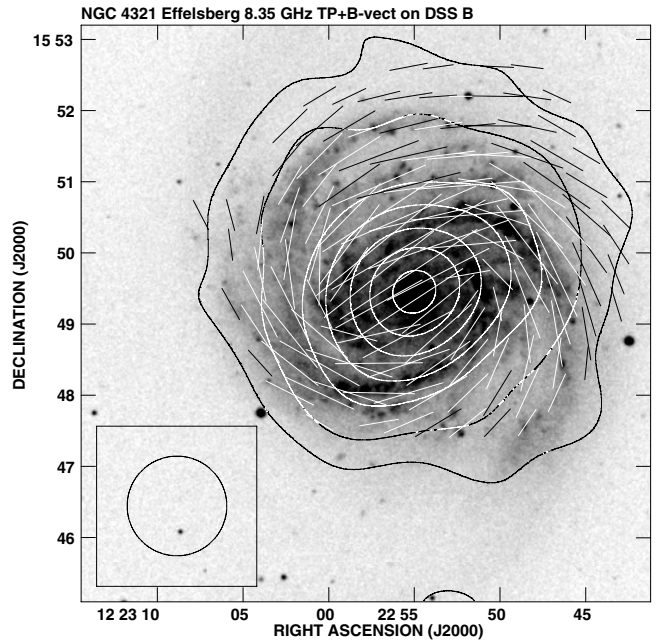


**Fig. 10.** Total power map of NGC 4321 at 8.35 GHz with apparent *B*-vectors of polarized intensity overlaid on the DSS blue image. The contours are 3, 8, 16, 25, 40, 55, 70 × 0.3 mJy/b.a., and a vector of 1′ length corresponds to the polarized intensity of 0.5 mJy/b.a. The map resolution is 1.′5. The beam size is shown in the *bottom left* corner of the figure.

Virgo cluster outskirts. This relatively unperturbed galaxy shows a faint H I tail extending to the southwest (Knapen 1992).

The total power emission (Fig. 10) is roughly symmetric with however slightly more extensions to the north. It is consistent with the observations of Urbanik et al. (1986) at 10.7 GHz.

The disk contains three radio sources. Two of them were identified in the NVSS as J122258 + 155052 and J122251 + 154941 with the total fluxes at 1.49 GHz of 41.2 mJy and 79.8 mJy, respectively. The third source, cataloged by the NVSS as J122258 + 154828 with the total flux of 55.7 at 1.49 GHz, is
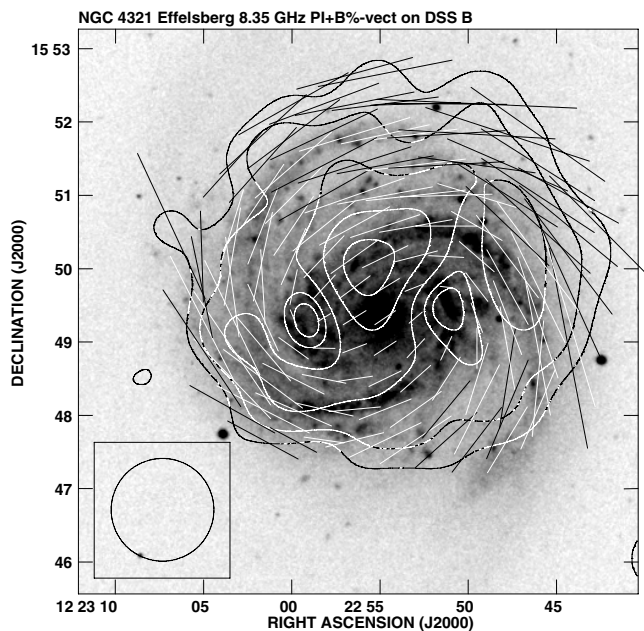
**Fig. 11.** Map of polarized intensity of NGC 4321 at 8.35 GHz with apparent *B*-vectors of polarization degree overlaid on the DSS blue image. The contours are 3, 5, 8, 12, 16 × 0.07 mJy/b.a., and a vector of 1′ length corresponds to the polarization degree of 10%. The map resolution is 1′.5. The beam size is shown in the *bottom left* corner of the figure.



**Fig. 12.** Map of the rotation measure between 4.85 GHz and 8.35 GHz of NGC 4321. The contours are −10, −5, −3, 0, 3, 5, 10 × 20 rad/m². The map resolution is 2′.5. The beam size is shown in the *bottom left* corner of the figure.



**Fig. 13.** Total power map of NGC 4388 at 4.85 GHz with apparent *B*-vectors of polarized intensity overlaid on the DSS blue image. The contours are 3, 10, 25, 40, 60, 70 × 0.9 mJy/b.a., and a vector of 1′ length corresponds to the polarized intensity of 0.5 mJy/b.a. The map resolution is 2′.5. The beam size is shown in the *bottom right* corner of the figure.

the supernova 1979C (Weiler et al. 1980), which is clearly visible in the maps of Urbanik et al. (1986) but at present seems to be much weaker, with the flux density of only about 6 mJy at 1.49 GHz, hence fainter by almost 90% (Soida, priv. comm.). The total power peak coincides with the optical center of the galaxy.

The apparent polarization *B*-vectors closely follow the optical spiral structure, especially in the central parts of the galaxy, which hosts a distinct bar. The peak of polarized intensity is shifted northwards from the center with the emission forming an S-shape structure in the central parts of the disk following the spiral structure (Fig. 11). The emission minima visible at both ends of the bar are due to beam depolarization. The highest polarization degree (up to 30%) can be found in the northwestern part of the disk, where an H I ridge was reported (Cayatte et al. 1990).

### 3.5. NGC 4388

NGC 4388 is a Seyfert 2 Sb-type spiral galaxy located close to the cluster core at the distance of only 1°.3 (390 kpc in the sky plane) from Virgo A. The H I observations of Oosterloo & van Gorkom (2005), as well as Hα observations of Veilleux et al. (1999) and Yoshida et al. (2004) suggest that this galaxy is heavily stripped and highly deficient in H I, forming a 100 kpc long tail, and that the observed Hα outflow is most likely a partial ionisation of this tail by an active nuclei of the galaxy.

The total power emission (Fig. 13) is dominated by the central region of the galaxy (over 119 mJy at 1.4 GHz) and by two NVSS radio background sources placed symmetrically on both sides of the galaxy center (J122551 + 123951 and J122540 + 123958 with total flux densities of 4 mJy and 7.9 mJy respectively). The low surface-brightness extension to the west is very likely a mixture of the NVSS radio background source
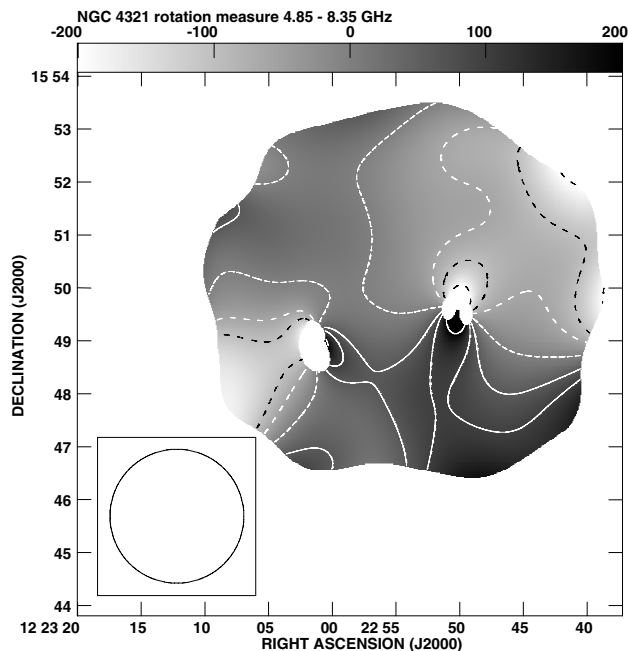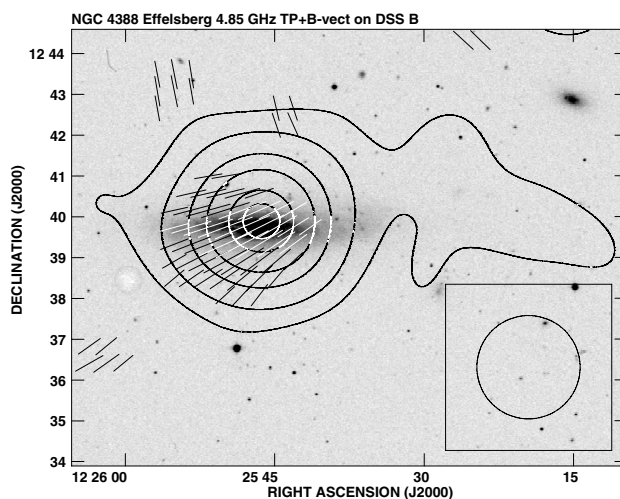
J122528+124111 with a total flux density of 2.5 mJy at 1.4 GHz and FIRST radio background source J122519.2+123854 with a total flux density of 13.05 mJy at 1.4 GHz. However, the northern part of this extension (around RA$_{2000}$ = 12$^h$25$^m$27$^s$, Dec$_{2000}$ = 12°41′30″) does not correspond to any radio background source. It remains unclear whether it might be real emission associated with the galaxy.

The apparent polarization *B*-vectors deviate significantly from the disk plane by about 30° and are roughly aligned with the direction towards the cluster core (M 87), forming a "polarized fan" (Vollmer et al. 2007). Our low-resolution observations allow us to detect low surface-brightness structures, which is
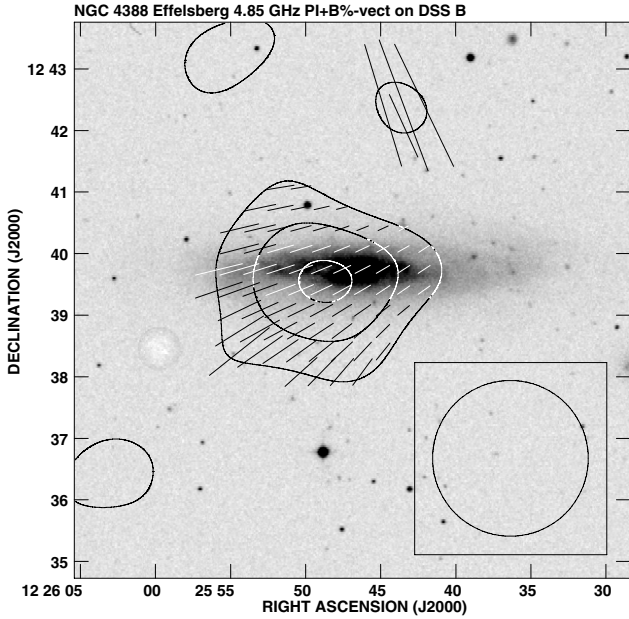
**Fig. 14.** Map of polarized intensity of NGC 4388 at 4.85 GHz with apparent *B*-vectors of polarization degree overlaid on the DSS blue image. The contours are 3, 5, 7 × 0.1 mJy/b.a., and a vector of 1′ length corresponds to the polarization degree of 3.75%. The map resolution is 2′.5. The beam size is shown in the *bottom right* corner of the figure.

even more important in the case of a significantly stripped galactic disk. Our studies clearly show that the magnetic-field ordering occurs globally.

### 3.6. NGC 4535

NGC 4535 is a grand-design spiral galaxy located in the southern Virgo cluster subcluster that has formed around the giant elliptical M 49. The distance to the cluster core is 4°.3 (1.29 Mpc in the sky plane).

Optical images show the very regular spiral structure of NGC 4535, which also has a quite symmetric and extended H I distribution (Chung al. 2009). This is reflected in the symmetric distribution of the total intensity, whose peak is roughly situated at the galaxy center (Fig. 15).

Our observations at 8.35 GHz (Fig. 16) confirm our previous findings at lower resolution (see Weżgowiec et al. 2007), that the asymmetry of the polarized emission is significant and remains at a similar level (73% compared to 75% at 4.85 GHz). Therefore, the asymmetry cannot be caused by the large beam. The peak of the polarized emission is located in the western optical spiral arm. This agrees with observations by Vollmer et al. (2010), who found a similar enhancement in the polarized radio emission.

The apparent polarization *B*-vectors generally follow the spiral structure. The degree of polarization varies across the disk from 15% in the eastern disk half to 30% in its western half, reaching 40% in the western outskirts of the optically visible galaxy.

### 3.7. Faraday rotation

For all galaxies except NGC 4388, observations at two frequencies (4.85 GHz and 8.35 GHz) were used (for 6 cm observations of NGC 4535, see Weżgowiec et al. 2007) to derive rotation measure maps (Figs. 3, 6, 9, 12, and 17) allowing the
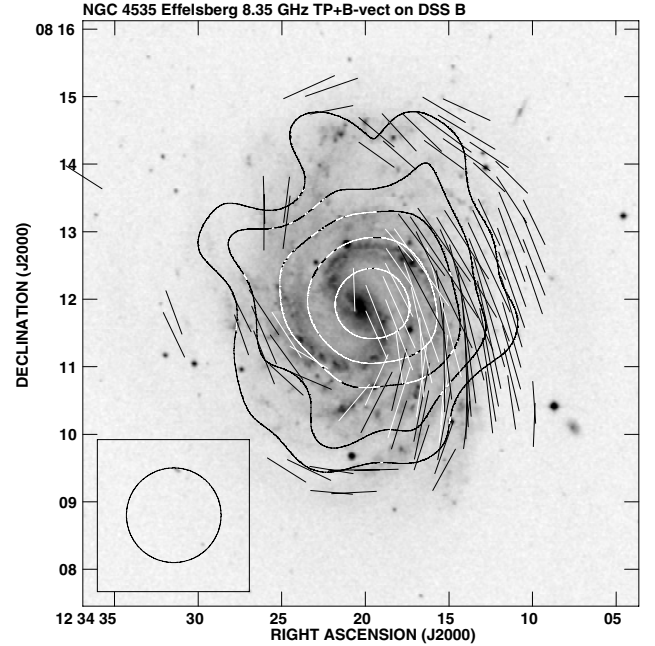
**Fig. 15.** Total power map of NGC 4535 at 8.35 GHz with apparent *B*-vectors of polarized intensity overlaid on the DSS blue image. The contours are 3, 5, 8, 12, 17 × 0.3 mJy/b.a., and a vector of 1′ length corresponds to the polarized intensity of 0.3 mJy/b.a. The map resolution is 1′.5. The beam size is shown in the *bottom left* corner of the figure.
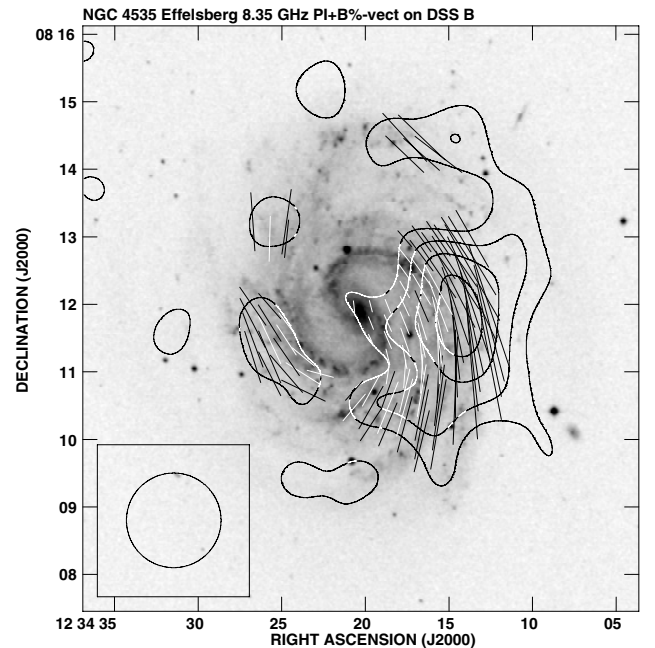
**Fig. 16.** Map of polarized intensity of NGC 4535 at 8.35 GHz with apparent *B*-vectors of polarization degree overlaid on the DSS blue image. The contours are 3, 5, 7, 9 × 0.07 mJy/b.a., and a vector of 1′ length corresponds to the polarization degree of 20%. The map resolution is 1′.5. The beam size is shown in the *bottom left* corner of the figure.

determination of mean Faraday rotation between those two frequencies. The high-frequency maps were convolved to the resolution at 4.85 GHz.

Since we only use two frequencies, we need to take into account possible contributions from the galactic ISM, as well as from the cluster ICM and the Galactic foreground, to investigate whether there is a *n-π* ambiguity problem typical of the Faraday
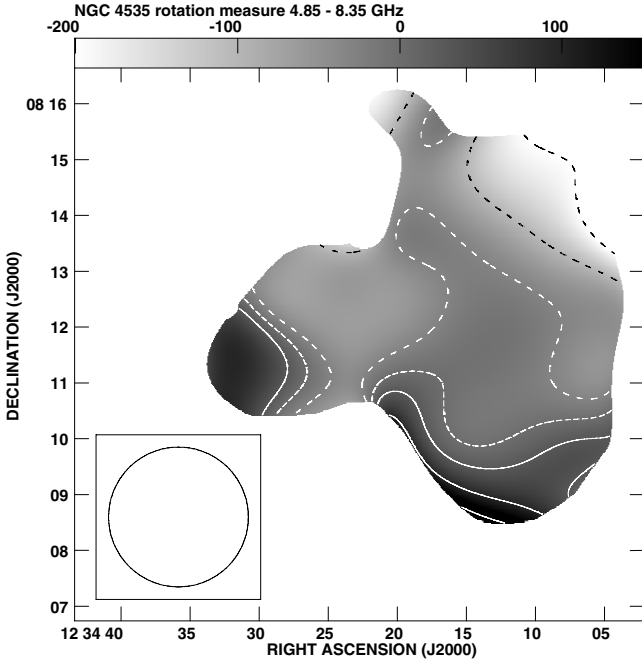
**Fig. 17.** Map of the rotation measure between 4.85 GHz and 8.35 GHz of NGC 4535. The contours are $-20, -10, -3, 0, 3, 10, 20 \times 10$ rad/m$^2$. The map resolution is $2\rlap{.}'5$. The beam size is shown in the *bottom left* corner of the figure.

rotation (Rudnick et al. 2011). As a typical ISM rotation measure in spiral galaxies, we assume $\pm 50$ rad/m$^{-2}$ (Beck 2002), which makes them "Faraday thin" at the observed wavelengths. To check whether the contribution of the external screen can be a problem, we used the rotation measure measurements by Taylor et al. (2009) in the direction of the galaxies included in this study. Although these measurements can also be affected by the ICM, for the purpose of this paper we do not intend to separate its contribution from that of the Galaxy and use the total values only. In all cases, we found extreme values of the rotation measures not exceeding $\pm 30$ rad/m$^{-2}$, which correspond to the rotation of the polarization plane by $\pm 6$ degrees at 4.85 GHz and $\pm 2$ degrees at 8.35 GHz. Since the rotation measure maps were calculated with polarization angle maps clipped at $3\sigma$ in polarized emission, we expect a maximum uncertainty in the rotation measure of $\sim 20$ rad/m$^{-2}$. Taking into account the flux uncertainties in our maps and the large beam of our observations, we conclude that the Faraday rotation introduced by the external screen is still within the errors of our analysis. Consequently, we assume that our results are unaffected by n-pi ambiguity.

Because of the limited resolution of our study, the detailed analysis of the rotation measure distributions is impossible, as we have only few beams per galaxy, which makes it possible to easily cancel out any gradients. Examination of the maps shows that the average rotation measures agree with the values obtained by Taylor et al. (2009) in the direction to the Virgo cluster.

Although our observations allow us to study only the total rotation measures along the line-of-sight, for the two almost face-on galaxies, NGC 4303 and NGC 4321 (Figs. 9 and 12, respectively), we may detect a significant contribution to the rotation measures from the disk magnetic field, as we observe large-scale rotation-measure patterns that are symmetric with respect to the disk center. This can hardly be generated in the ICM and may be attributed to the component of the disk field along the line-of-sight. We tried to fit single ($\sin(\phi)$)

and double-periodic ($\sin(2\phi)$) curves to the azimuthal rotation-measure variations in NGC 4303 and NGC 4321. The profiles of those variations were constructed using the *sector* task of the NOD2 package, by integrating the $Q$ and $U$ signals in concentric rings within the galactic disk. Unfortunately, no statistically good fits were possible. Hence, the patterns of the regular fields in these galaxies are more complicated than single axisymmetric or bisymmetric spirals. We note here that our conclusion should be confirmed with higher resolution observations.

## 4. Discussion

We now attempt to categorize the observed effects exerted on particular galaxies by the cluster environment. While these effects are caused by the different processes governing the interactions, these effects reflect the influence of the cluster environment upon the galaxies.

An alternative explanation of the observed radio polarized intensity distributions in Virgo cluster spiral galaxies was given by Pfrommer & Dursi (2010), who claim that they may be the result of the draping of the cluster magnetic field that is oriented radially. Although we agree that, since the cluster is filled with magnetized plasma, such draping of the cluster field most likely occurs, we argue that the distributions of the radio polarized intensity in Virgo spiral galaxies are related to their evolution within the cluster environment. In this paper, Weżgowiec et al. (2007), and Vollmer et al. (2007), these distributions closely agree with the simulations of Vollmer (2009) and the observations in H I (Chung et al. 2007), suggesting that the observed radio polarized features, along with the disturbed neutral gas morphologies, result from either ram-pressure or tidal-interaction effects. If the radio polarized ridges observed in Virgo cluster spirals reflected only the cluster field, we would most likely observe mainly unperturbed galactic disks with symmetric magnetic fields. The examples of perturbed galactic disks and their magnetic fields presented below clearly contradict this scenario.

### 4.1. Asymmetric halo in edge-on galaxies

By observing asymmetries in both the total power and polarized emission of edge-on galaxies, we are able to trace possible extensions outside the galaxy plane. We can thus examine the effects of the cluster environment on the magnetic fields in the halo. The location of NGC 4192 in the cluster outskirts does not suggest that there have been any strong interactions with the dense ICM. Nevertheless, although the galaxy is not H I deficient, the significant asymmetry of both the total and polarized radio emission visible in our maps may suggest that some interactions with the environment might have occured. This may be similar to the case of another Virgo cluster galaxy – NGC 4402, where strong ram pressure effects are clearly visible (see Crowl et al. 2005; Vollmer et al. 2007). Moreover, the X-shaped structure of the magnetic field vectors alignment in NGC 4192, similar to those frequently found in edge-on spirals (Tüllmann et al. 2000; Soida et al. 2011), is visible only on the western side, as in NGC 4402. Its lack on the eastern side may also signify, together with the total power asymmetry, that there have been some external perturbations. It is possible that we see a slight compression of the eastern side of the disk due to ram pressure effects, in which case this would be the leading edge of the galaxy.

In contrast to NGC 4192, the observations of NGC 4388 presented in Sect. 3.5 (Figs. 13 and 14) reveal a strong global asymmetry of the magnetic field with most of the polarized emission coming from the eastern and southeastern parts of this galaxy.

A similar asymmetry was found by Vollmer et al. (2007). His high resolution observations show the complex structure of the magnetic field, but do not allow us to study global asymmetries owing to the possible missing flux.

We assume that our observations are insignificantly affected by the high rotation-measure produced in the cluster medium and/or our Galaxy, as discussed in Sect. 3.7. Despite the low resolution of the observations, they show the overall properties of the magnetic field, such as its global inclination to the galactic plane. The asymmetry of the polarized intensity, which has a higher polarization degree in the south and apparent polarization *B*-vectors aligned in the southeast-northwest direction, suggest that the galaxy is moving in the southwestern direction, as concluded by Yoshida et al. (2004) from the H$\alpha$ outflow alignments and their spectral analysis. This also seems to be confirmed by the X-ray data presented by Weżgowiec et al. (2011), who detected an extended hot gas tail corresponding to a long H I tail found by Oosterloo & van Gorkom (2005).

The main cause of the differences in the morphologies of NGC 4388 and NGC 4192 is most likely their different distances from the cluster core. While the former is situated in the central parts of the cluster and is undoubtely affected by the high density ICM environment, the latter is in the remote regions of the cluster, where the density of the ICM is relatively low. A H I deficiency can clearly be seen for both galaxies – only 0.18 in the outskirts NGC 4192 and 0.84 for the core galaxy NGC 4388 (Cayatte et al. 1990). As we argue above, our observations suggest that there has been some degree of interaction between NGC 4192 and the surrounding environment. We probably observe an early stage of the cluster influence exerted on this galaxy, when the magnetic field structure only begins to be slightly distorted with no significant gas deficiency being present. It is possible that the future of this galaxy will be similar to what we observe in the case of NGC 4388, which is nearly devoid of a gaseous disk and whose magnetic field seems to be strongly affected by the harsh cluster core conditions. The density of the ICM, as well as the intensity of the interactions between galaxies, reach their highest values at the cluster core. A similar trend is found for the velocities of the galaxies, as core galaxies tend to move faster than outskirts ones.

### 4.2. Collisional compressions?

In a dense cluster environment, tidal interactions are more common than those between field galaxies. This may also be the case for NGC 4302 and NGC 4298. An eastern extension from NGC 4302 up to 2′ (10 kpc in the sky plane) followed by the apparent *B*-vectors together with a peak in the polarized intensity that is shifted towards NGC 4298 may suggest that both galaxies constitute a physical pair, especially as their difference in radial velocity is only about 14 km s$^{-1}$. Most of the polarized emission is located in the region between the galaxies, where the highest polarization degree is observed. A similar case was observed in NGC 4038/4039 by Chyży & Beck (2004), who argued that in this pair of interacting galaxies the regular magnetic field was amplified in the compression region between the galaxies. Our beam is too large to investigate the magnetic fields of NGC 4302 and NGC 4298 in such detail. Nevertheless, we found that the global distribution of the polarized emission resembles roughly that in NGC 4038/4039. Therefore, we find it very likely that there is a region of compressed magnetic fields *between* NGC 4302 and NGC 4298 resembling that in the NGC 4038/4039 system, and especially that the degree of polarization is higher in the region between

NGC 4298 and NGC 4302 reaching ≃15% compared to ≃10% in the region between NGC 4038 and NGC 4039. Nevertheless, the latter pair is observed shortly after the encounter, while NGC 4302 and NGC 4298 are most likely approaching the phase of an encounter, making them more similar to the pair NGC 876/NGC 877 (Drzazga et al. 2011), which are at roughly the same stage of interaction.

Chung et al. (2007) reported a mild truncation of the H I disk of NGC 4302 together with a gas tail extending to the north. The H I disk of NGC 4298 is shifted to the northwest and the stellar disk extends to the southeast. However, they found none of the significant neutral-hydrogen emission between both galaxies usually seen in interacting pairs, which is a surprising result. It could be possibly explained by an early stage of interactions. High resolution polarimetric observations of NGC 4302 and NGC 4298 would be desirable, especially of the latter galaxy, since with our large beam we cannot detect polarized intensity owing to beam depolarization effects.

### 4.3. Distributions in the disk plane

As reported in Weżgowiec et al. (2007), in the case of NGC 4535, which is a grand-design spiral galaxy located in the southern outskirts of the Virgo cluster, the high asymmetry of the polarized emission is fairly unexpected and suggests that there has been strong external gas compression. Observations with a 1′.5 resolution presented in this paper, as well as those of Vollmer et al. (2007, 2010), confirm our previous findings from the data made with a resolution of 2′.5. However, a deep H I survey of the Virgo cluster spiral galaxies (VIVA, Chung et al. 2009) shows that the polarized radio ridge still lies within an extended H I envelope around NGC 4535 as presented by Vollmer et al. (2010). Therefore, the significant enhancement of the magnetic field and an extended polarized radio ridge in the outskirts of the optical galactic disk could be explained by shearing forces instead of external compressions.

Two other spiral galaxies in the cluster outskirts do not seem to be influenced by the surrounding environment, which is what we expect considering their distance from the cluster core. The first of the two is NGC 4303 in the southern outskirts of the cluster, which is even further away from the cluster core than NGC 4535 (the distance to the cluster core is 8°.2 and 4°.3, respectively). It is also a grand-design spiral, whose symmetric distribution of polarized intensity is not indicative of any significant interaction. However, a slight increase in the polarization degree, thus a higher degree of magnetic field ordering, in the eastern disk, as well as the higher pitch angle of the magnetic field, may represent some external influence. In particular, the X-ray observations of Tschöke et al. (2000) trace central activity that may be triggered by tidal interactions within the cluster environment. Likely evidence of this could be a radio emission extension to the northeast. In addition, the presence of close companions – NGC 4301 (about 9.8′ = 49 kpc in the sky plane – northeast of NGC 4303) and NGC 4292 (about 12.2′ = 61 kpc – in the sky plane to the northwest) – suggests that there may be interactions in the future.

For both NGC 4303 and NGC 4535, even moderate resolution data provides evidence of "magnetic arms", where the spiral structure of the regular fields is concentrated in the interarm regions (as seen in NGC 6946 by Beck et al. 2007). This however would require confirmation with higher resolution observations.

Similarly to NGC 4303, in NGC 4321, another grand-design spiral galaxy, located in the northern outskirts of

the Virgo cluster, a higher degree of polarization is seen on one side (northern) of the disk. This and a faint H I tail extending to the southwest, which is accompanied by a large-scale distortion of the H I field found by Knapen (1992), favor the same tidal interaction scenario. This scenario is also supported by the presence of close companions (NGC 4322, 5′.3 to the north, and NGC 4328, 6′.1 to the east with a faint visible bridge connecting the latter to NGC 4321).

Such significant differences in the magnetic field distributions of galaxies in the cluster outskirts suggest that the degree of distortions in a galactic magnetic field is not a simple function of the distance to the cluster center (see Table 1). However, bearing in mind that the magnetic disturbances can be "remembered" by the galaxy for hundreds of Myr (Otmianowska-Mazur & Vollmer 2003), we are aware that the observed situation may not reflect present interactions. We would then conclude that the cluster outskirts galaxies are generally weakly perturbed and that any objects bearing strong signs of distortions are merely the "products" of earlier interactions close to the cluster center. Nevertheless, there is still a possibility that, under certain conditions of a velocity in a direction against the ICM, even lower density of the latter would produce such strong distortions in an outskirts galaxy. A more obvious situation is that represented by NGC 4303 and NGC 4321, which lack any signs of perturbations. These regularly looking galaxies with homogenous H I distributions have very likely orbited the cluster at large distances from its center or, more probably, are relatively new members of the cluster. In the latter case, we could be observing NGC 4303 and NGC 4321 in the pre-stripping stage of evolution.

On the other hand, face-on galaxies that look unperturbed might be in fact distorted in the $z$-direction, which is suggested by a complex configuration of their magnetic fields (see Sect. 3.7). The angle $\Theta$ between the velocity vector $\boldsymbol{v}$ and the rotation vector $\boldsymbol{\Omega}$ of a galaxy is then an important quantity. It may be a general parameter describing the level of distortions in the galactic magnetic fields by either ram pressure or shearing effects, a level that obviously does not depend on the distance of a galaxy from the cluster center. The highest asymmetries of the magnetic field in face-on galaxies should be visible when $\Theta = 90°$, as may be the case for NGC 4535. For NGC 4303 and NGC 4321, $\Theta$ could be $\simeq 0°$, which would ensure that any shifts in the $z$-direction would be undetectable.

### 4.4. Global properties of cluster galaxies

As we present above, cluster galaxies tend to be disturbed. To check how this influences their disk emission, we construct a plot comparing the radio and far-infrared surface brightnesses of all 12 Virgo cluster galaxies from our study with the radio – far-infrared (FIR) correlation for non-cluster nearby galaxies. The method used here is described in Weżgowiec et al. (2007). This plot is presented in Fig. 18. As in our previous studies (see also Weżgowiec et al. 2007), almost all galaxies follow the correlation very well. We performed a Kolmogorov-Smirnov test to compare the distribution of q for our cluster and non-cluster samples of spirals. The obtained probability p-value was 0.33, which suggests that there are no significant statistical differences between both samples.

Spiral galaxies with active nuclei (NGC 4438 – see Weżgowiec et al. 2007, and NGC 4388) seem to have some excess of radio emission above that expected from the FIR brightness. NGC 4388, a heavily stripped galaxy, does not deviate above the correlation as much, as in the case of NGC 4438, though the radio excess is clearly visible. This
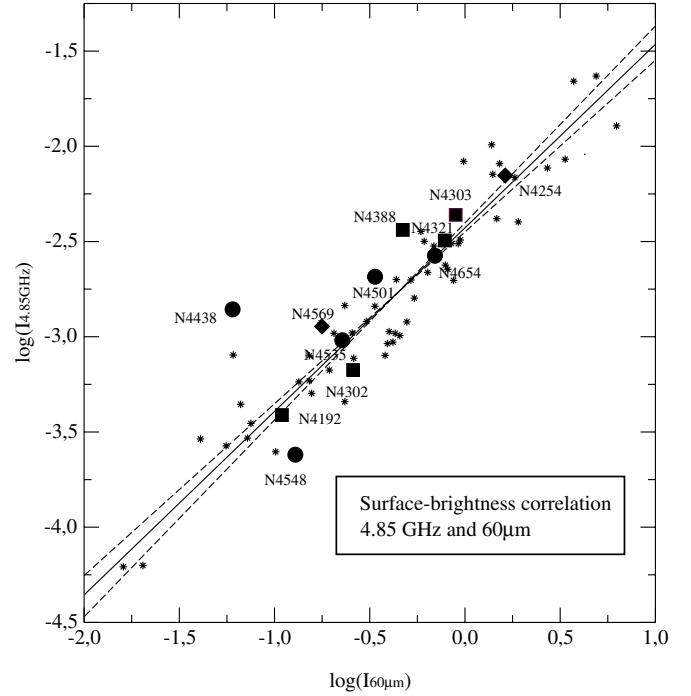


**Fig. 18.** Radio – FIR diagram for our Virgo objects plotted as symbols with labels and for the reference sample of galaxies observed by Gioia et al. (1982) with an extension towards low surface-brightness objects observed by Chyży et al. (2006) – both as dots. The surface brightness at 4.85 GHz (Jy/□′) and at 60 $\mu$m (Jy/□′, see text) is used. The solid curve is an orthogonal fit to reference non-cluster galaxies with a slope of $0.96 \pm 0.06$. The dashed lines show the "regression scissors", the maximum and minimum slopes (1.03 and 0.90) allowed by the data scatter.

highly gas-deficient galaxy also possesses an active nucleus (Seyfert 2), which may contribute to the radio emission regardless of gas abundance and star formation. Nevertheless, almost all galaxies from our sample (except the discussed examples and NGC 4548 – see Weżgowiec et al. 2007) show that even strongly perturbed galaxies closely follow the radio – FIR correlation. This may be explained by the external perturbations being able to increase both the radio and far-infrared emission by triggering enhanced star-formation.

Although of low resolution, our radio data can provide some clues about the global configuration of the magnetic field in our sample galaxies. A high mean value of rotation-measure in NGC 4192 can show that for this galaxy a large foreground rotation may be introduced by the cluster medium. NGC 4303 and NGC 4321 most likely have complex magnetic-field structures, as we were unable to fit either single or double-periodic curves to the azimuthal rotation-measure variations. Nevertheless, we note that these suggestions need to be confirmed by a detailed analysis of high-resolution rotation-measure data.

## 5. Summary and conclusions

We have presented results of the second part of our systematic study of the magnetic-field structures of Virgo cluster spirals (see also Weżgowiec et al. 2007). As previously, we used the Effelsberg radio telescope at 4.85 GHz to detect the weak, extended total power and polarized emission, and particular objects

were studied in more detail at 8.35 GHz. Our studies yielded the following results:

– In the edge-on galaxies NGC 4192 and NGC 4388, we found asymmetric halos, which in the latter galaxy is heavily distorted.
– NGC 4302 likely forms a physical pair with a close companion NGC 4298. The asymmetries of the polarized intensity together with Hα asymmetries and H I tails support this scenario. Between the galaxies, there is a region of polarized emission that, as in the case of NGC 4038/4039, indicates that the magnetic field has been amplified by tidal interactions between both objects.
– Our higher resolution observations of NGC 4535 presented here confirm the strong asymmetry of the polarized emission and enhancement of the magnetic field found in Weżgowiec et al. (2007). Since this feature lies within the extended H I envelope (see Vollmer et al. 2010, it is most likely caused by shearing forces.
– Two outskirts face-on galaxies have different radio-emission distributions. While NGC 4303 seems completely unperturbed, NGC 4321 shows signs of perturbations. This may mean that the degree of distortion of a galaxy is not a simple function of its distance from the cluster center.
– The magnetic fields of both NGC 4303 and NGC 4321 have symmetric spiral patterns, whereas that of NGC 4535 is highly asymmetric.
– The perturbations of the galactic stellar or ISM component or both do not significantly affect the radio – far infrared correlation. The only exception in our sample introduced in this paper was NGC 4388, which displays only a slight excess of radio emission most likely due to active galactic nucleus (AGN) activity. In Weżgowiec et al. (2007), we found a more significant excess in another AGN host – NGC 4438.
– The angle $\Theta$ between the velocity vector $\boldsymbol{v}$ and the rotation vector $\boldsymbol{\Omega}$ of a galaxy may be a general parameter that describes the level of distortions in the galactic magnetic fields.

The "magnetic diagnostics" presented in this paper have been proven to trace environmental effects experienced by cluster galaxies interacting with either each other or the hot ICM. It provides us with a very sensitive tool for examining perturbations sometimes not yet visible in other domains. Even low-resolution but sensitive observations of the polarized intensity may yield some clues about the magnetic-field configuration via a rotation-measure analysis. Encouraged by the results of this and our previous work, we plan to extend our sample even further to obtain polarized intensity data for radio-weaker galaxies, located in different parts of the cluster. This would allow us to perform an extensive statistical study of the effects of various kinds of interactions upon the properties of galaxies. This will also be done by combining our data with available data in X-rays, H I,

Hα, and CO. We expect this study to provide comprehensive insight into the evolution of galaxies in a particularly "influential" environment.

## References

Baars, J. W. M., Genzel, R., Pauliny-Toth, I. I. K., & Witzel, A. 1977, A&A, 61, 99
Beck, R. 2002, ASP Conf. Ser., 275, 331
Beck, R. 2007, A&A, 470, 539
Beck, R., Fletcher, A., Shukurov, A., et al. 2005, A&A, 444, 739
Cayatte, V., van Gorkom, J. H., Balkowski, C., & Kotanyi, C. 1990, AJ, 100, 604
Cayatte, V., Kotanyi, C., Balkowski, C., & van Gorkom, J. H. 1994, AJ, 107, 1003
Chemin, L., Balkowski, C., Cayatte, V., et al. 2006, MNRAS, 366, 812
Chung, A., van Gorkom, J. H., Kenney, J. D. P., & Vollmer, B. 2007, ApJ, 659, 115
Chung, A., van Gorkom, J. H., Kenney, J. D. P., et al. 2009, AJ, 138, 1741
Chyży, K. T., & Beck, R. 2004, A&A, 417, 541
Chyży, K. T., Urbanik, M., Soida, M., & Beck, R. 2002, A&AS, 281, 409
Chyży, K. T., Soida, M., Bomans, D. J., et al. 2006, A&A, 447, 465
Chyży, K. T., Bomans, D. J., Krause, M., et al. 2007, A&A, 462, 933
Crowl, H. H., Kenney, J. D. P., van Gorkom, J. H., & Vollmer, B. 2005, AJ, 130, 65
Condon, J. J., Cotton, W. D., Greisen, E., et al. 1998, AJ, 115, 1693
Drzazga, R. T., Chyży, K. T., Jurusik, W., & Wiórkiewicz, K. 2011, A&A, 533, A22
Gioia, I. M., Gregorini, L., & Klein, U. 1982, A&A, 116, 164
Knapen, J. H. 1992, PhDT, 209
Koopmann, R. A., & Kenney, J. D. P. 2004, ApJ, 613, 866
Oosterloo, T., & van Gorkom, J. 2005, A&A, 437, 19
Otmianowska-Mazur, K., & Vollmer, B. 2003, A&A, 402, 879
Paturel, G. 2003, A&A, 412, 45
Pfrommer, C., & Dursi, J. L. 2010, Nature, 6, 520
Roediger, E., & Brüggen, M. 2008, MNRAS, 388, 465
Rudnick, L., Brown, S., & Farnsworth, D. 2011, Mem. Soc. Astron. Italiana, 82, 551
Schulz, S., & Struck, C. 2001, MNRAS, 328, 185
Soida, M., Urbanik, M., & Beck, R. 1996, A&A, 312, 409
Soida, M., Krause, M., Dettmar, R.-J., & Urbanik, M. 2011, A&A, 531, A127
Taylor, A. R., Stil, J. M., & Sunstrum, C. 2009, ApJ, 702, 1230
Tschöke, D., Hensler, G., & Junkes, N. 2000, A&A, 360, 447
Tüllmann, R., Dettmar, R.-J., Soida, M., et al. 2000, A&A, 364, L36
Urbanik, M., Klein, U., & Gräve, R. 1986, A&A, 166, 107
Veilleux, S., Bland-Hawthorn, J., & Cecil, G. 1999, AJ, 118, 2108
Vollmer, B. 2009, A&A, 502, 427
Vollmer, B., Cayatte, V., Balkowski, C., & Duschl, W. J. 2001, ApJ, 561, 708
Vollmer, B., Beck, R., Kenney, J. D. P., & van Gorkom, J. H. 2004, AJ, 127, 3375
Vollmer, B., Soida, M., Beck, R., et al. 2007, A&A, 464, 37
Vollmer, B., Soida, M., Chung, A., et al. 2010, A&A, 512, A36
Weiler, K. W., van der Hulst, J. M., Sramek, R. A., & Panagia, N. 1980, BAAS, 12, 752
Weżgowiec, M., Urbanik, M., Vollmer, B., et al. 2007, A&A, 471, 93
Weżgowiec, M., Vollmer, B., Ehle, M., et al. 2011, A&A, 531, A44
Yoshida, M., Ohyama, Y., Iye, M., et al. 2004, AJ, 127, 90